

## Slight La doping induced ferromagnetic clusters in layered $\text{La}_{3-3x}\text{Sr}_{1+3x}\text{Mn}_3\text{O}_{10}$ ( $x=1.00, 0.99, 0.95$ )

Yan-kun Tang, Xiao Ma, Zhi-qi Kou, Young Sun, Nai-li Di, Zhao-hua Cheng, and Qing-an Li\*  
*State Key Laboratory of Magnetism, Institute of Physics, Chinese Academy of Sciences, Beijing 100080, China*  
 (Received 1 May 2005; revised manuscript received 6 July 2005; published 6 October 2005)

The magnetic properties of the layered manganites  $\text{La}_{3-3x}\text{Sr}_{1+3x}\text{Mn}_3\text{O}_{10}$  with  $x=1.00, 0.99,$  and  $0.95$  have been studied by dc and ac magnetization as well as specific heat measurements. For  $x=1.00$ , the magnetization shows a broad peak centered around 160 K, which is due to a short-range low-dimensional antiferromagnetic ordering. Below  $T_N=67$  K where the anomaly of magnetic specific heat is observed, the system possibly develops into a long-range three-dimensional antiferromagnetic ordering. The anisotropic magnetic interactions between Mn ions are responsible for the temperature-dependent spin ordering. For  $x=0.99$  and  $0.95$ , the slight doping of La leads to significant changes in magnetic properties. The zero-field cooled and field cooled magnetization, ac susceptibility, as well as isothermal  $M$ - $H$  curves suggest that La doping induces ferromagnetic clusters in the antiferromagnetic matrix. The shift of the specific heat peak indicates that the antiferromagnetic coupling in the matrix is weakened due to La doping.

DOI: [10.1103/PhysRevB.72.132403](https://doi.org/10.1103/PhysRevB.72.132403)

PACS number(s): 75.50.Ee, 75.40.Cx, 75.50.Lk

Perovskite manganites have been constantly in the limelight during the past decade since the discovery of the colossal magnetoresistance (CMR) effects. A large amount of research activity has been performed on manganese oxides  $(R,A)_{n+1}\text{Mn}_n\text{O}_{3n+1}$  with Ruddlesden-Popper (RP) structure.<sup>1</sup> For the  $n=3$  compounds, some detailed works were reported about  $\text{Ca}_4\text{Mn}_3\text{O}_{10}$  which belongs to RP phase.<sup>2</sup> However, attempts to prepare  $\text{Sr}_4\text{Mn}_3\text{O}_{10}$  and  $\text{Ba}_4\text{Mn}_3\text{O}_{10}$  resulted in a new layered phase.<sup>3,4</sup> The two oxides, isotypic to  $\text{Ba}_4\text{TiPt}_2\text{O}_{10}$ ,<sup>5</sup> crystallize in the  $Cmca$  space group and are built up from  $\text{Mn}_3\text{O}_{12}$  trimers of three sharing-faces octahedra. These trimers are linked through common vertices to form corrugated sheets perpendicular to the  $b$  axis of the orthorhombic unit cell, and Sr (Ba) atoms occupy the space between the layers. The magnetic and structural properties of polycrystalline  $\text{Ba}_4\text{Mn}_3\text{O}_{10}$  have been studied carefully by neutron diffraction, specific heat, and magnetization measurements.<sup>4,6</sup> A broad maximum, probably caused by short-range spin pairing within the layers, was observed in the susceptibility at 130 K.<sup>4</sup> Long-range antiferromagnetic (AFM) ordering seems to occur below 80 K.<sup>6</sup> Up to date, the work about  $\text{Sr}_4\text{Mn}_3\text{O}_{10}$  is concerned with the structure<sup>3,7,8</sup> whereas little information on the magnetic properties is available.

In this paper, we have carried out an investigation of magnetic properties and specific heat of  $\text{La}_{3-3x}\text{Sr}_{1+3x}\text{Mn}_3\text{O}_{10}$  ( $x=1.00, 0.99, 0.95$ ). Our study indicates that  $\text{Sr}_4\text{Mn}_3\text{O}_{10}$  is an AFM insulator with  $T_N=67$  K and slight electron-doping leads to significant change in the magnetic properties due to the formation of FM clusters. Polycrystalline samples were synthesized by the standard method of solid state reaction in air. A stoichiometric mixture of  $\text{SrCO}_3$ ,  $\text{MnCO}_3$ , and  $\text{La}_2\text{O}_3$  powders was well ground and calcined twice at 900 °C and 950 °C for 24 h. Then, the resulting powder was pressed into pellets and sintered at 1150 °C, 1160 °C, and 1250 °C for 24 h, respectively. The phase purity and crystal structure of the samples were examined by powder x-ray diffraction (XRD). Data were collected by step scanning over the angu-

lar range  $10^\circ \leq 2\theta \leq 80^\circ$  and analyzed by the Rietveld method implemented in the program Rietica.<sup>9</sup> The dc magnetization was measured using a SQUID magnetometer. The specific heat and ac magnetization were measured using a Quantum Design PPMS.

XRD patterns of our samples are identical to the data collected by Floros *et al.*<sup>3</sup> The structure (see the inset of Fig. 1) was refined in the space group  $Cmca$ , adopting the published  $\text{Sr}_4\text{Mn}_3\text{O}_{10}$  crystal structure data as the starting point.<sup>3</sup> Strontium and lanthanum cations were assumed to be

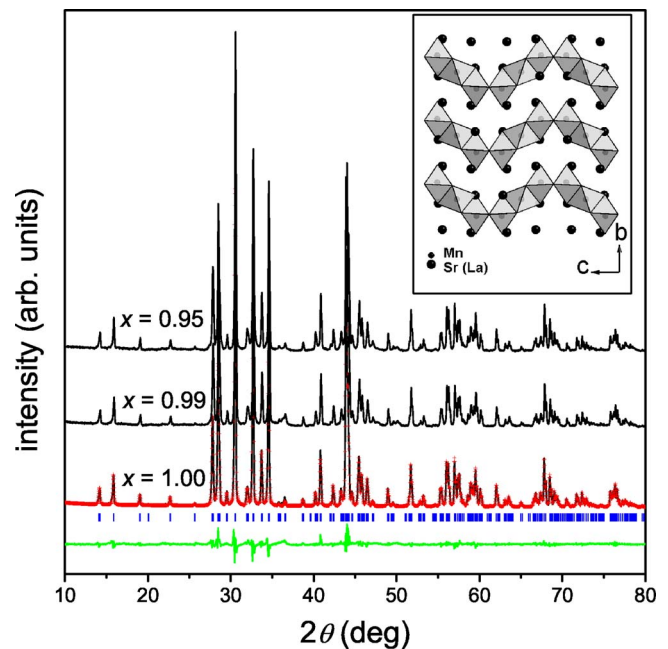


FIG. 1. (Color online) XRD patterns of  $\text{La}_{3-3x}\text{Sr}_{1+3x}\text{Mn}_3\text{O}_{10}$  ( $x=1.00, 0.99, 0.95$ ) at room temperature. The calculated (dots) and difference (bottom line) data of  $x=1.00$  and the positions of the Bragg reflections (small vertical lines) are also shown. The inset shows the  $[100]$  projection of the crystal structure.

TABLE I. Structural parameters of  $\text{La}_{3-3x}\text{Sr}_{1+3x}\text{Mn}_3\text{O}_{10}$  ( $x=1.00, 0.99, 0.95$ ).

$x$	1.00	0.99	0.95
$a$ (Å)	5.4740(1)	5.4751(1)	5.4762(1)
$b$ (Å)	12.4573(2)	12.4577(3)	12.4557(3)
$c$ (Å)	12.5249(2)	12.5291(3)	12.5313(3)
Mn 1-Mn 2 (Å)	$2.510(2) \times 2$	$2.513(3) \times 2$	$2.518(3) \times 2$
$R_p$ (%)	4.74	5.76	6.23
$R_{wp}$ (%)	6.42	8.12	8.29
$\chi^2$	3.45	5.41	5.45

statistically distributed over the same crystallographic sites. Figure 1 shows the XRD patterns of three samples. The final structural parameters are listed in Table I. The fitting results show that no trace of the secondary phase is detected at room temperature for  $x \geq 0.95$ . We also attempted to synthesize  $x < 0.95$  samples. However, no single-phase samples were obtained based on the XRD patterns that show extra diffraction peaks. As shown in Table I, La doping only enlarges the  $c$  parameter slightly, which indicates that the interplane distance is much less affected by the doping of La than the intraplane distance. The average Mn—Mn distances in the  $\text{Mn}_3\text{O}_{12}$  trimers are slightly elongated with the La increment.

Figure 2 shows the temperature dependence of the zero-field-cooled (ZFC) and field-cooled (FC) magnetization in 1000 Oe for the three samples. For  $x=1.00$  sample, the magnetization exhibits a broad peak centered around 160 K and rises sharply below 40 K. The broad peak in  $M(T)$  is characteristic of low dimensional antiferromagnetically coupled spin systems,<sup>2</sup> and suggests that this is not a transition from a high temperature paramagnetic state to a low temperature three-dimensional (3D) AFM state. Assuming that there is low dimensional AFM structure, we may express  $M(T)$  as a sum of three components,

$$M(T)/H = \chi_{\text{BF}}(T) + \chi_{\text{LT}}(T) + \chi_{\text{vV}}(T). \quad (1)$$

$\chi_{\text{BF}}(T)$  is the Bonner-Fisher susceptibility of a one-dimensional (1D) antiferromagnetic spin chain,<sup>10,11</sup>

$$\chi_{\text{BF}}(T) = \frac{N_A \mu_{\text{eff}}^2}{3k_B T} \frac{0.25 + 0.14995x + 0.30094x^2}{1 + 1.9862x + 0.68854x^2 + 6.0626x^3}, \quad (2)$$

with  $x = |J|/k_B T$ . The  $\chi_{\text{LT}}(T)$  is a Curie-like term at low temperature,

$$\chi_{\text{LT}}(T) = \frac{C}{T + \theta}. \quad (3)$$

$\chi_{\text{vV}}(T)$  is a temperature-independent Van-Vleck susceptibility. The fitting curve with Eq. (1) is shown as a solid line in Fig. 2(a) with parameters  $\mu_{\text{eff}} = 6.40\mu_B$  and  $J = 200$  K. The experimental data cannot be fitted perfectly by Eq. (1), which indicates that the structure of  $\text{Sr}_4\text{Mn}_3\text{O}_{10}$  is not equivalent to a 1D-AFM spin chain. However, the fit does support the picture of low dimensional antiferromagnetically coupled

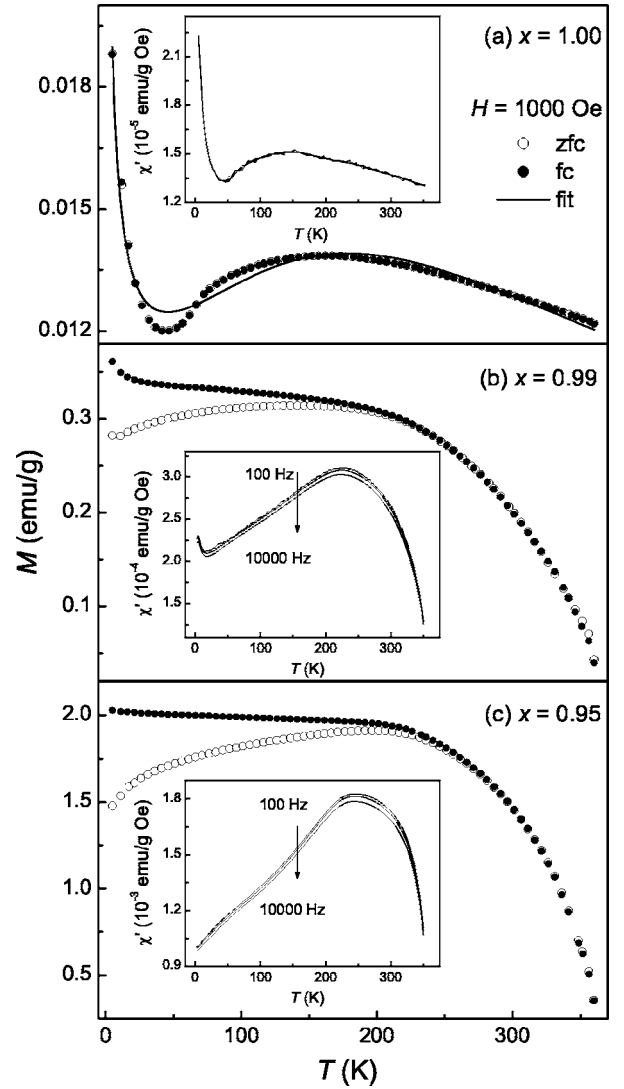


FIG. 2. FC and ZFC dc magnetization for samples  $\text{La}_{3-3x}\text{Sr}_{1+3x}\text{Mn}_3\text{O}_{10}$  ( $x=1.00, 0.99, 0.95$ ). The solid line is the fit of  $M(T)$  using Eq. (1). The insets show the ac susceptibility for all samples.

spin system for  $x=1.00$  sample. By fitting the  $M(T)$  curve at the high temperature region ( $220 \text{ K} \leq T \leq 360 \text{ K}$ ) with Curie-Weiss law, we obtain  $\theta = -960$  K;  $\mu_{\text{eff}} = 5.14\mu_B$  per Mn. Although the negative  $\theta$  value strongly supports the existence of strong AFM interactions, the  $\mu_{\text{eff}}$  value is much larger than the theoretical effective moment of the  $\text{Mn}^{4+}$  free ion ( $3.87\mu_B$ ). Therefore, there should exist some short-range magnetic interaction at temperatures up to 360 K. The Curie-type upturn of  $M(T)$  below 50 K is peculiar. However, similar results were recently observed in other low dimensional AFM systems, which have been attributed to a staggered field effect.<sup>12,13</sup>

The  $M(T)$  curves of  $x=0.99$  and  $0.95$  samples, shown in Fig. 2(b) and Fig. 2(c), are quite different from that of  $x=1.00$  sample. The shape of the two curves displays ferromagnetism-like behavior. The magnetic moment increases with the doping of La. There is a big diverge between ZFC and FC data below an irreversibility temperature about

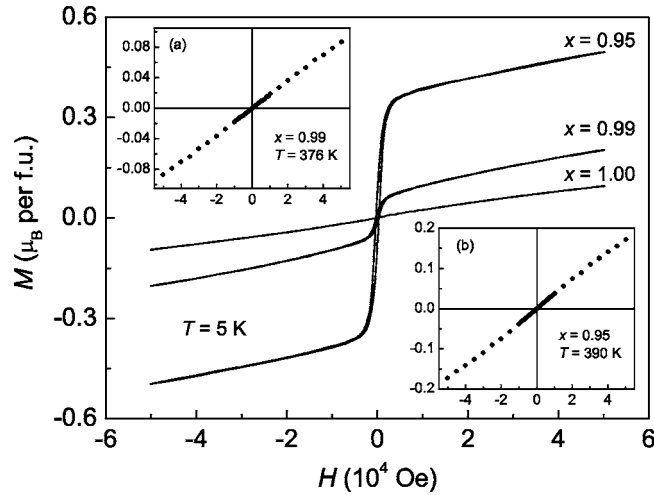


FIG. 3. The dc magnetization as a function of field of  $\text{La}_{3-3x}\text{Sr}_{1+3x}\text{Mn}_3\text{O}_{10}$  ( $x=1.00, 0.99, 0.95$ ), measured at 5 K. The insets show  $M$  vs  $H$  at 376 K and 390 K for  $x=0.99$  and  $x=0.95$ , respectively.

230 K and 255 K in  $x=0.99$  and  $x=0.95$ , respectively. These behaviors indicate that either inhomogeneous clusters or homogeneous spin-glass phase is induced by La doping.

To clarify this point, we studied the ac susceptibility for all samples as shown in the insets of Fig. 2, measured in zero dc field, with an alternating field  $H_{ac}=10$  Oe and frequencies of 100, 1000, and 10 000 Hz. For  $x=1.00$  sample, a broad peak centered around 160 K and an upturn at low temperature are observed, which is analogous to the dc magnetization. No frequency dependency is observed. For  $x=0.99$  and 0.95 samples, the two samples show a peak around 220 K and 240 K, corresponding to the irreversibility temperature in the  $M(T)$  curves. The peak reduces at lower frequencies. These features are characteristic of a spin-glass phase or an inhomogeneous clustered system. However, the broad peak and the slight variation of the  $\chi'$  peak temperature with frequency are qualitatively different from the behavior of typical spin glasses which usually show narrow cusp and obvious variation of the  $\chi'$  peak temperature with the frequency.<sup>14</sup> Therefore, it is more likely that there exist FM clusters embedded in the AFM matrix for  $x=0.99$  and  $x=0.95$  samples. The gradual freezing of the FM clusters moments with decreasing temperature results in the broad peak in susceptibility.

To further confirm the magnetic structure of the samples, we also measured isothermal  $M$  vs  $H$  curves at 5 K as plotted in Fig. 3. For the  $x=1.00$  sample,  $M$  increases almost linearly with  $H$ . For the La doped samples, magnetization rises sharply with the increase of field. Hysteresis is observed at  $H < 5000$  Oe and the magnetization does not saturate even in 5 T. Taking into account the fact that hysteresis appears even at high field for spin glass, it is more likely that La doping results in FM clusters rather than a spin-glass phase. The FM clusters are embedded in an AFM matrix. Through running the  $M(H)$  curves at different temperatures we found that the  $M(H)$  curve becomes linear and hysteresis disappears above 376 K and 390 K for  $x=0.99$  and  $x=0.95$ , respectively, as shown in the inset (a) and (b) of Fig. 3. These

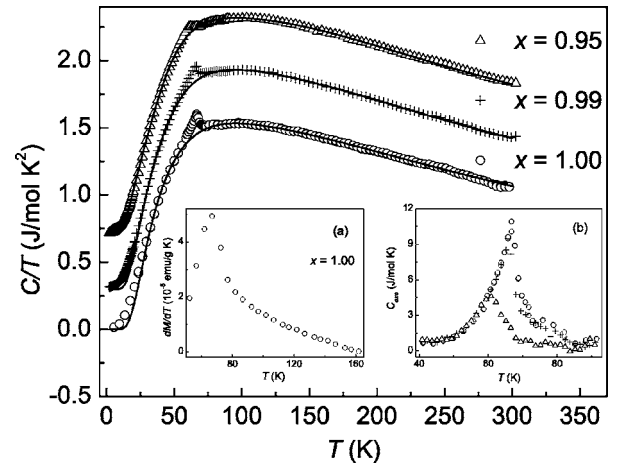


FIG. 4. Temperature dependence of the specific heat for  $\text{La}_{3-3x}\text{Sr}_{1+3x}\text{Mn}_3\text{O}_{10}$  ( $x=1.00, 0.99, 0.95$ ). The solid line is the fitting of the lattice background to the Einstein model. For clearness, the  $x=0.99$  and  $x=0.95$  curves were shifted upward by  $0.3 \text{ J/mol K}^2$  and  $0.7 \text{ J/mol K}^2$ , respectively. Inset (a) the derivative of the magnetization of  $x=1.00$  around 70 K. Inset (b)  $C_{exc}$  vs  $T$  around  $T_N$  for  $\text{La}_{3-3x}\text{Sr}_{1+3x}\text{Mn}_3\text{O}_{10}$  ( $x=1.00, 0.99, 0.95$ ).

temperatures may correspond to the Curie temperature of the minor FM clusters for  $x=0.99$  and  $x=0.95$ , respectively.

The combined analysis of  $M(T)$  and  $M(H)$  does not provide complete understanding about these samples' magnetic properties. To resolve the ambiguity in the magnetic measurements we have measured specific heat for all samples (Fig. 4). A peak is clearly observed at  $T=67$  K for  $x=1.00$ . The inset (a) of Fig. 4 shows the temperature derivative of the magnetization vs temperature, and a cusp around  $T=67$  K is also detected. This coincidence indicates that this temperature is a critical point, below which it is likely that  $x=1.00$  presents a long-range three-dimensional AFM order. Previous investigations on  $\text{Ba}_4\text{Mn}_3\text{O}_{10}$  reported similar coincidence at  $T=80$  K, and this temperature has been further confirmed as Néel temperature ( $T_N$ ) by neutron diffraction data.<sup>6</sup> The specific heat curves for  $x=0.99$  and 0.95 samples are similar to that for  $x=1.00$  sample. A cusp is also observed at 65 K and 61 K, respectively, and no other anomaly is visible over the whole experimental temperature. Thus we can conclude that the two samples are not spin-glass systems. The major magnetic phases of them are still similar to the magnetic phase of  $x=1.00$  sample. Meanwhile, the minor FM clusters are formed with the doping of La. In addition, the cusp gradually shifts toward the low temperature as La content increases. In order to investigate the nature of the magnetic transition at  $T_N$ , we must first estimate the lattice contribution to the specific heat. Then the magnetic specific heat can be obtained by subtracting the lattice contribution. We have obtained the lattice contribution  $C_{\text{lattice}}$  by fitting  $C$  in the interval from 30 K to 220 K using Einstein model given by

$$C_{\text{Einstein}} = 3nR \sum_i a_i \left( \frac{x_i^2 e^{x_i}}{(e^{x_i} - 1)^2} \right), \quad (4)$$

where  $x_i = T_i/T$ . The calculated  $C_{\text{lattice}}$  is then extrapolated to the whole experimental temperature region. After the estima-

tion of the lattice contribution, we define  $C_{\text{exc}}$  as

$$C_{\text{exc}} = C - C_{\text{lattice}}. \quad (5)$$

Thus obtained  $C_{\text{exc}}$  close to  $T_N$  was plotted in the inset (b) of Fig. 4. It is obvious that the magnitude of anomaly decreases and the anomaly shifts toward the low temperature side as  $x$  decreases. The dwindling of the anomaly suggests that the proportion of AFM phase reduces. The shift of the anomaly, similar to that in  $\text{Ca}_{1-x}\text{La}_x\text{MnO}_3$  and  $\text{Ca}_{1-n}\text{Tb}_n\text{MnO}_3$ ,<sup>15,16</sup> suggests that AFM couple is weakened due to the increment of La.

The AFM structure in  $x=1.00$  sample and the FM clusters induced by the doping of La may be related to the structure of these samples. According to the different environment of Mn ions, there should be three types of magnetic interactions. These interactions include a strong intratrimer interaction within  $\text{Mn}_3\text{O}_{12}$  trimers, an intertrimer interaction inside the ac layer and an interlayer interaction among the layers. For  $x=1.00$  sample, the spin pairing resulted from the intratrimer interaction is formed even at high temperature  $T=360$  K. With decreasing temperature the intratrimer coupling become stronger and the spin pairing continuously extends over a large temperature range. Thus the large effective

moment reflecting the existence of short-range order is obtained on the basis of Curie-Weiss law. The analogous spin pairing was reported in many manganese oxides built up from the units of face-sharing  $\text{MnO}_6$  octahedra, such as  $\text{Sr}_7\text{Mn}_4\text{O}_{15}$  and  $\text{Ba}_4\text{Mn}_3\text{O}_{10}$ .<sup>6,17</sup> With cooling the intertrimer interaction is large enough to grow the magnetic clusters. These clusters seem to be two-dimensional short-range order. Finally, the interlayer interaction is so strong that a long range 3D AFM ordering is possibly established below 67 K, where both the peak of the specific heat and the peak of the derivative of the magnetization are observed. For La doped samples, the magnetic behavior is similar to  $x=1.00$  sample. On the other hand,  $\text{Mn}^{3+}$  ions are created from  $\text{Mn}^{4+}$ . Double exchange coupling between  $\text{Mn}^{3+}$  and  $\text{Mn}^{4+}$  leads to FM clusters around  $\text{Mn}^{3+}$  sites. Because the little amounts of La and the anisotropic coupling, the doped electrons appear to remain essentially localized. As a result, there is no long-range FM ordering but the presence of FM clusters embedded in an AFM matrix. This picture is similar to that in  $\text{Ca}_{1-x}\text{R}_x\text{MnO}_3$  and  $\text{R}_{0.08}\text{Ca}_{1.92}\text{MnO}_4$ .<sup>15,18</sup>

This work was supported by the State Key Project of Fundamental Research, and the National Natural Sciences Foundation of China.

\*Corresponding author. Electronic address: qali@aphy.iphy.ac.cn

<sup>1</sup>Y. Moritomo, A. Asamitsu, H. Kuwahara, and Y. Tokura, *Nature* (London) **380**, 141 (1996).

<sup>2</sup>J. Lago, P. D. Battle, and M. J. Rosseinsky, *J. Phys.: Condens. Matter* **12**, 2505 (2000).

<sup>3</sup>N. Floros, M. Hervieu, G. V. Tendeloo, C. Michel, A. Maignan, and B. Raveau, *Solid State Sci.* **2**, 1 (2000).

<sup>4</sup>V. G. Zubkov, A. P. Tyutyunnik, I. F. Berger, V. I. Voronin, G. V. Bazuev, C. A. Moore, and P. D. Battle, *J. Solid State Chem.* **167**, 453 (2002).

<sup>5</sup>H. Blattner, H. Gränicher, W. Känzig, and W. Merz, *Helv. Phys. Acta* **21**, 341 (1948).

<sup>6</sup>K. Boulahya, M. Parras, J. M. González-Calbet, U. Amador, J. L. Martínez, and M. T. Fernández-Díaz, *Phys. Rev. B* **69**, 024418 (2004).

<sup>7</sup>J. Fabry, J. Hybler, Z. Jirak, K. Jurek, K. Maly, M. Nevřiva, and V. Petricek, *J. Solid State Chem.* **73**, 520 (1988).

<sup>8</sup>H. J. Rossell, P. Goodman, S. Bulcock, R. H. March, S. J. Kennedy, T. J. White, F. J. Lincoln, and K. S. Murray, *Aust. J. Chem.* **49**, 205 (1996).

<sup>9</sup>C. J. Howard and B. A. Hunter, *A Computer Program for Rietveld*

*Analysis of X-Ray and Neutron Powder Diffraction Patterns* (Lucas Heights Research Laboratories, NSW, Australia, 1998).

<sup>10</sup>Jill C. Bonner and Michael E. Fisher, *Phys. Rev.* **135**, A640 (1964).

<sup>11</sup>William E. Hatfield, *J. Appl. Phys.* **52**, 1985 (1981).

<sup>12</sup>R. Feyherm, S. Abens, D. Günther, T. Ishida, M. Meißner, M. Meschke, T. Nogami, and M. Steiner, *J. Phys.: Condens. Matter* **12**, 8495 (2000).

<sup>13</sup>E. E. Kaul, H. Rosner, V. Yushankhai, J. Sichelschmidt, R. V. Shpanchenko, and C. Geibel, *Phys. Rev. B* **67**, 174417 (2003).

<sup>14</sup>J. A. Mydosh, *Spin Glasses: An Experimental Introduction* (Taylor and Francis, London, 1993).

<sup>15</sup>A. L. Cornelius, B. E. Light, and J. J. Neumeier, *Phys. Rev. B* **68**, 014403 (2003).

<sup>16</sup>Y. Moritomo, A. Machida, E. Nishibori, M. Takata, and M. Sakata, *Phys. Rev. B* **64**, 214409 (2001).

<sup>17</sup>J. F. Vente, K. V. Kamenev, and D. A. Sokolov, *Phys. Rev. B* **64**, 214403 (2001).

<sup>18</sup>C. Autret, C. Martin, R. Retoux, A. Maignan, B. Raveau, G. André, F. Bourée, and Z. Jirak, *J. Magn. Magn. Mater.* **284**, 172 (2004).